

Sintering and Characterization of a Transparent Ferroelectric NaNbO_3 Ceramic

X. Lin, Z.-F. Li*, L.-F. Shu

College of Materials Science and Engineering, China Jiliang University, Hangzhou 310018, P. R. China
received October 21, 2016; received in revised form December 28, 2016; accepted February 8, 2017

Abstract

NaNbO_3 transparent ceramics were prepared with a delicately controlled solid state reaction method. The structures and properties of the samples were determined using X-ray diffraction (XRD), scanning electron microscope (SEM), ferroelectric hysteresis loops and UV-Vis spectroscopy. The XRD results showed that the antiferroelectric *Pbcm* and ferroelectric *R3c* phases coexist in NaNbO_3 ceramics. In SEM images, the NaNbO_3 ceramics presented a compact microstructure with fewer pores among its grains, enhancing its light transmission and weakening its absorption and reflection, which was confirmed with UV-Vis spectroscopy. The high transparency of the NaNbO_3 ceramic was approximately 95 % for ultraviolet light and up to 97 % for visible light with a wavelength of more than 450 nm, corresponding to the band gap of 2.76 eV. The tunic-shaped hysteresis loops of the NN ceramic indicated that two phases co-contributed to its ferroelectricity. A high storage energy density of 650.40 kJ/m³ and breakdown voltage of 17.00 kV/mm were obtained. NaNbO_3 transparent ceramics therefore have practical applications in capacitors for energy storage.

Keywords: Transparent ceramics, NaNbO_3 , transmission, ferroelectric properties

I. Introduction

Over the past few decades, conventional optical transparent materials, such as glasses and polymers, have been widely used in modern industry. However, the limitations and deficiencies of these materials become obvious when their poor mechanical strength and unstable physical and chemical properties are considered. Moreover, these materials cannot normally maintain their optical performance in certain extreme conditions, like high temperature, high pressure, strong corrosion, etc. To combat these problems, scientists have tried to find alternative materials with both high transparency and improved performance. R. L. Coble *et al.*¹ from the General Electric Company first proposed the concept of transparent ceramics and successfully synthesized translucent aluminium oxide ceramics in the 1950s. The invention of transparent ceramics was a major breakthrough in the development of ceramics, as up until then ceramics were traditionally considered to be opaque. In the half-century since, scientists have successfully synthesized transparent oxide ceramics (Y_2O_3 , ZrO_2 , CaO , etc.)^{2,3}, composite oxide ceramics (like MgAl_2O_4 and $\text{Y}_3\text{Al}_5\text{O}_{12}$)^{4,5} and non-oxide ceramics (ZnS , CdTe , AlN)^{6,7}. Thanks to the development of preparation technologies, the optical properties of transparent ceramics are now comparable with those of glass. Ceramics are therefore regarded as a promising material for a wide range of applications, such as lighting devices, radio electronics, military applications, etc.

Sodium niobate NaNbO_3 (NN) ceramic is a conventional functional ceramic material, well known for its antifer-

roelectricity (AFE) in the broad range of temperatures between -100°C and 360°C ^{8,9}. It also exhibits outstanding dielectric and piezoelectric properties, thereby attracting much attention. In view of the scientific importance of NN ceramic, it is worth synthesizing transparent NN ceramic rather than others. Combining transparency with these properties will open up more applications such as photonic applications^{10,11,12} or electro-optic effect devices^{13,14} for such a high-quality transparent ceramic.

Hot-pressing and sintering and molten salt synthesis methods are commonly adopted to synthesize transparent ceramics^{15,16}. But the presence of a large number of pores makes ceramics opaque^{17,18,19}. For transparent NN ceramic, excessively high temperature may cause the volatilization of the alkali metal Na, resulting in the formation of undesirable secondary phases^{20,21,22}. Specifically, the conventional solid state reaction process has not been preferentially utilized for producing NN ceramic, although it presents the simplest and most economical method. In this work, the sintering process is conducted under carefully controlled conditions of sintering temperature and heat preservation to reduce porosity and enhance transparency. After preparation, X-ray diffraction (XRD) is used to detect the crystal structure of the NN ceramic, and UV-Vis spectroscopy is carried out to characterize the transparency of the NN ceramic with calculation of the band gap. The microstructures of the NN grains are imaged by means of a scanning electron microscope (SEM), and the physical properties of the material such as ferroelectric behaviour, storage energy density and

* Corresponding author: lizhengfa@cjlu.edu.cn

breakdown voltage are investigated to determine factors for designing optoelectronic devices.

II. Experimental Procedure

High-purity Na_2CO_3 (99.8 %, Yongda Chemicals, Tianjin, China) and Nb_2O_5 (99.5 %, Guoyao Chemicals, Shanghai, China) were used as raw materials. These were dried, weighed and mixed with a molar stoichiometric ratio of 1:1. The mixture was then ground for 24 h by means of ball-milling in an ethanol medium. After the addition of PVA (polyvinyl acetate) AH-26 adhesive (15 %, Huarui Chemicals, Hangzhou, China) to the ultra-fine powder and mixing, the powders were cold-pressed into pellets with a diameter of 15 mm under a pressure of 440 MPa using a wafer (YP-8T, China). The binder was then removed at 650 °C for 2 h and the pellets were sintered at a temperature of 1150 °C for 16 h to the maximum contraction of their diameters in an air atmosphere in a box furnace (Thermo Scientific, Lindberg/Blue, United States). Finally, after the pellets had been fully polished for 1 h, platinum electrodes were applied on both sides of the pellet by means of sintering at 900 °C for 1 h.

The NN ceramic was characterized with XRD on a Philips X'pert XRD system with CuK_α radiation. The microstructure and grain size distribution of the sintered samples were determined using a scanning electron microscope (JSM-6490F, Japan). UV-Vis spectroscopy of the polished NN ceramic was performed with a UV-2550 (SHIMADZU, Japan) spectrometer. The polarization-electric field (P-E) loop was measured at room temperature at 100 Hz using a Sawyer-Tower circuit.

III. Results and Discussion

The X-ray diffraction pattern of the NaNbO_3 ceramic sintered at 1150 °C is shown in Fig. 1. S.K. Mishra *et al.*²³ also demonstrated that antiferroelectric phase *Pbcm* and ferroelectric phase *R3c* coexist in NN at around room temperature by means of neutron diffraction. With regard to this result, the peaks are indexed to orthorhombic and rhombohedral cells associated not only with the space group for *Pbcm* (No.33–1270) but also for *R3c* (No.85–0390), and compared with information obtained from the inorganic crystal structure database (ICSD), respectively, which indicates that the NN ceramic possesses two phases. The Miller indices of *Pbcm* and *R3c* are marked in the pattern, respectively. Predictably, the presence of *R3c* phase as well as *Pbcm* phase may have a big impact on the microstructure and properties.

The microstructure of the NN ceramic is shown in Figs. 2(a) and (b). According to Fig. 2(a), the grain sizes of NN are 1–5 μm with no pores observed from the surface of the NN ceramic. Usually, the surface of pores is an interface among grains with dramatically different optical characteristics, which intensely reflects and refracts light. No pore, no reflection and refraction. As shown in Fig. 2(b), the fracture is obviously transcrystalline through the grains with a few pores shown as the black areas, and the distribution of the NN grains is narrow, vastly improving its transparency. From the

SEM images, triangular stacked plates are clearly observed at the surface of the NN ceramic grains. The configuration shows that NN ceramic possesses high density after solid-state sintering, which can enhance its transparency. But in Fig. 2(b), a transcrystalline fracture among the grains can be observed, and this phenomenon can be attributed to the coexistence of two phases *R3c* and *Pbcm* in the sample, which is confirmed with its XRD pattern. As the two phases have a different crystal structure, neighbouring grains may grow as a result of different driving forces; therefore, the transcrystalline fracture shown in Fig. 2(b) can relieve internal stresses in the NN ceramic. On the other hand, the complex structure has an adverse impact on transparency because of light scattering and birefringence.

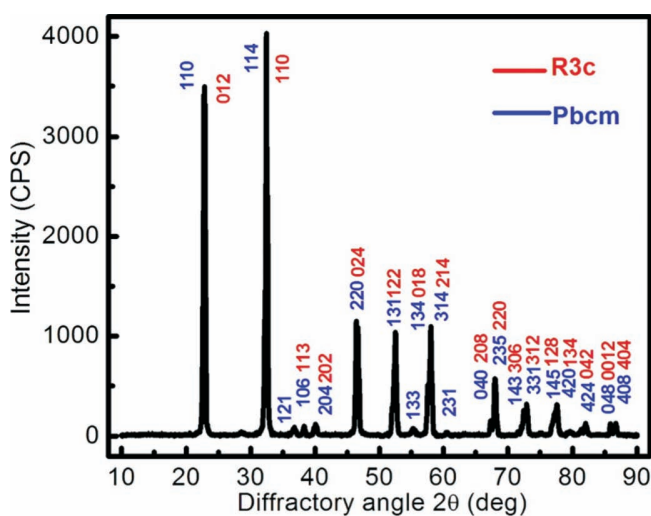


Fig. 1: XRD pattern of the NN ceramic at room temperature.

As shown in Fig. 3, ferroelectric hysteresis loops were measured under various electric fields. From Fig. 3, NaNbO_3 ceramic sintered at 1150 °C for 16 h presents an antiferroelectric-like hysteresis loop because of its tunic-shaped loops. The coercive electric field E_c and remnant polarization P_r of the NN ceramic is 3.23 kV/mm and 2.33 $\mu\text{C}/\text{cm}^2$, respectively. But for antiferroelectric materials, there should be a double hysteresis loop at room temperature. And the tunic-shaped loop may be attributed to the metastable state of the coexistence of antiferroelectric *Pbcm* and ferroelectric *R3c* phases in the NN^{24,25}, which was proved with the XRD results. From Fig. 3, the maximum storage energy density D_m of the NN ceramics can be calculated according to the following formula:

$$D_m = (\epsilon_0 E_m^2 + E_m P_m) / 2 \quad (\text{J}/\text{m}^3) \quad (1)$$

where E_m and P_m are the maximum values of the coercive electric field and polarization, respectively. After the measurement of hysteresis loops, the breakdown voltage was obtained under a high electric field. The high storage energy density ($D_m = 650.340 \text{ kJ}/\text{m}^3$) and breakdown voltage ($V_{br} = 17.00 \text{ kV}/\text{mm}$) of the NN ceramic make it a promising material in electronic devices, especially for the development of capacitors.

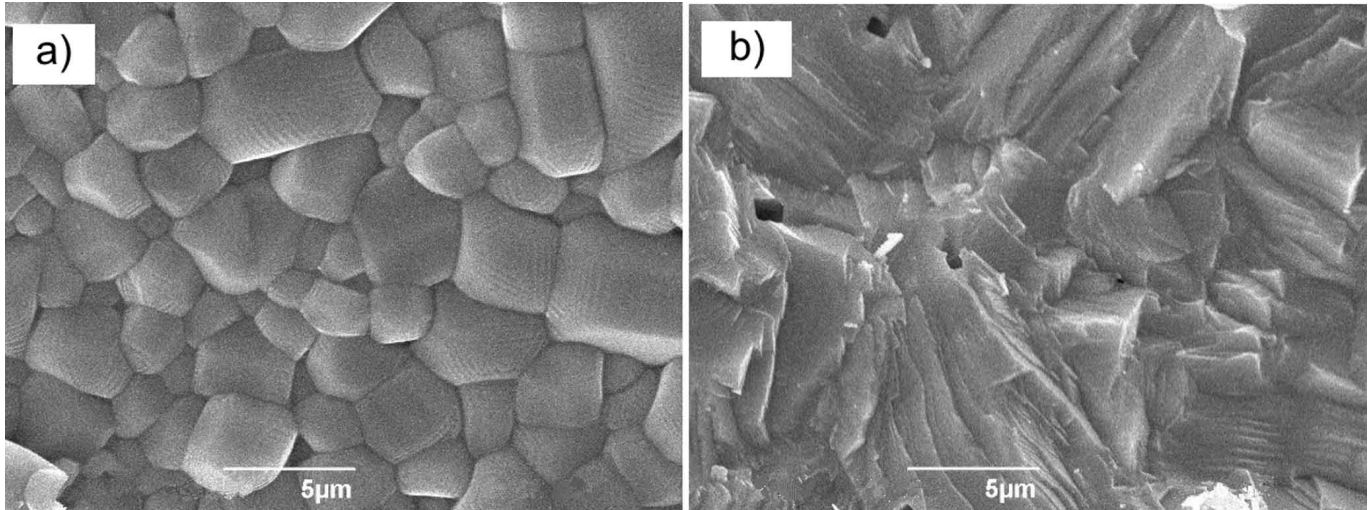


Fig. 2: SEM images of the NN ceramic sintered at 1150 °C: (a) natural and (b) fracture surfaces.

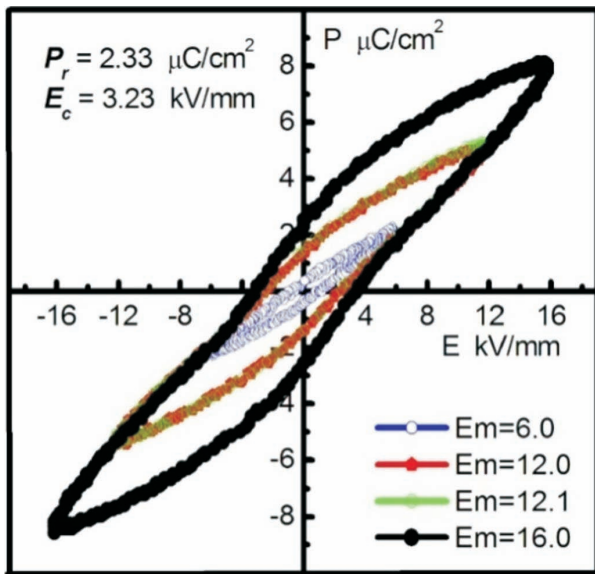


Fig. 3: Ferroelectric hysteresis loops of the unpoled NN ceramic.

Transparency of NaNbO₃ ceramics polished on both sides was investigated further with an UV-Vis spectrophotometer, and the absorption spectrum measured as shown in Fig. 4. To determine the absorption edge of the NN ceramic, the tangent line is adopted to assist the analysis in Fig. 4. Based on Fig. 4, there is a steady trend with the low absorptivity of 5.0 % in the range of 200–400 nm. It then shows a remarkable downward trend until around 450 nm, bottoming out at approximately 2.75 %. The result demonstrates that the NN ceramic exhibits high transparency for visible light, and the transmittances are more than 95 %. This may be attributable to the dense microstructure of NN ceramic, with fewer pores and defects thanks to the long-time heat preservation, as shown in Fig. 2, which can reduce the reflected light on grain boundaries. Additionally, the blue tangent line drawn along the falling curve intersects with the axis of wavelength at the threshold point of 450 nm, corresponding to the typical wavelength of blue light. The band gap can be calculated from the formula as follows ²⁶:

$$E_g = 1239.8 / \lambda_g \text{ (eV)} \quad (2)$$

where the λ_g is the wavelength corresponding to the point of intersection. The band gap of NN ceramic is calculated to be 2.76 eV, which is close to 2.95 eV of violet but far above that of red. It proves quantitatively that the NN ceramic presents a high transparent state. A word can be easily identified when read through the NN ceramic, which demonstrates the material’s high transparency. Confirmed with the XRD results for the NN ceramic, the two-phase coexistence is the main factor decreasing its transparency in Fig. 4.

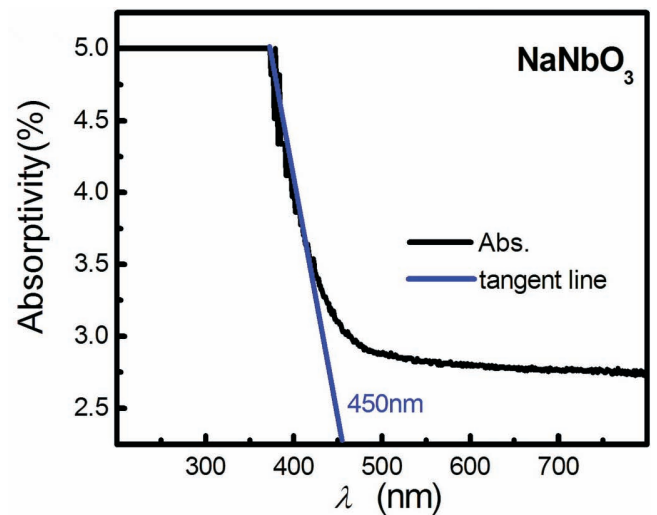


Fig. 4: Absorption spectrum of the NN ceramic sintered at 1150 °C.

IV. Conclusions

In summary, NaNbO₃ transparent ceramics were synthesized in a solid state reaction process. Delicate control of reaction conditions guarantees the high transparency of NN ceramic, which is detected by means of UV-Vis spectroscopy and photography. The coexistence of the antiferroelectric phase *Pbcm* and ferroelectric phase *R3c* in the NN ceramic confirmed by means of XRD directly affects both its microstructure and transparency. The tunica-shaped hysteresis loops of the NN ceramic, instead of the typical or double loops, indicate that two phases

can co-contribute to the ferroelectricity of NN ceramic at room temperature. Furthermore, the high storage energy density of 650.40 kJ/m³ and breakdown voltage of 17.00 kV/mm demonstrate that NN transparent ceramics have enormous potential in practical applications.

Acknowledgements

This work was supported by the Zhejiang Provincial Natural Science Foundation of China (Grant No. LY15A040004).

References

- Coble, R.L.: Transparent alumina and method of preparation. US, Patent Application (1962) 3,026,210.
- Saito, N., Matsuda, S., Ikegami, T.: Fabrication of transparent yttria ceramics at low temperature using carbonate-derived powder, *J. Am. Ceram. Soc.*, **81**, 2023–2028, (1998).
- Anselmi-Tamburini, U., Woolman, J.N., Munir, Z.A.: Transparent nanometric cubic and tetragonal zirconia obtained by high-pressure pulsed electric current sintering, *Adv. Funct. Mater.*, **17**, 3267–3273, (2007).
- Becher, P.F.: Press-forged Al₂O₃-rich spinel crystals for IR applications, *Am. Ceram. Soc. Bull.*, **56**, 1015, (1977).
- De, G., Dijk H.J.A.V.: Translucent Y₃Al₅O₁₂ ceramics, *Mater. Res. Bull.*, **19**, 1669–1674, (1984).
- Kim, Y.D., Sonezaki, K., Maeda, H., Kato, A.: Sintering behaviour of monodispersed ZnS powders, *J. Mater. Sci.*, **32**, 5101–5106, (1997).
- Kuramoto, N., Taniguchi, H.: Transparent AlN ceramics, *J. Mater. Sci. Lett.*, **3**, 471–474, (1984).
- Cross, L.E., Nicholson, B.J.: LV. the optical and electrical properties of single crystals of sodium niobate, *The London, Edinburgh, and Dublin philosophical Magazine and Journal of Science*, **46**, 453–466, (1955).
- Megaw, H.D.: The seven phases of sodium niobate, *Ferroelectrics*, **7**, 87–89, (1974).
- Yamane, M., Asahara, Y.: Glasses for photonics. Cambridge University Press. Cambridge (2000).
- Woggon, U.: Optical properties of semiconductor quantum dots, *Physics Today*, **117**, 217–222, (1997).
- Yu, D., Wang, C., Guyot-Sionnest, P.: N-type conducting CdSe nanocrystal solids, *Science*, **300**, 1277–80, (2003).
- Kong, L.B., Ma, J., Zhang, R.F., Zhang, T.S.: Fabrication and characterization of lead lanthanum zirconate titanate (PLZT7/60/40) ceramics from oxides, *J. Alloy. Compd.*, **339**, 167–174, (2002).
- Marssi, M.E., Farhi, R., Dellis, J.L., Glinchuk, M.D., Seguin, L., Viehland, D.: Ferroelectric and glassy states in La-modified lead zirconate titanate ceramics: A general picture, *J. Appl. Phys.*, **83**, 5371–5380, (1998).
- Cheng, Z., Ozawa, K., Miyazaki, A., Kimura, H.: Formation of lithium niobate from peroxide aqueous solution, *J. Am. Ceram. Soc.*, **88**, 1023–1025, (2005).
- Ge, H., Hou, Y., Xia, C., Zhu, M., Wang, H., Yan, H.: Preparation and piezoelectricity of NaNbO₃ high-density ceramics by molten salt synthesis, *J. Am. Ceram. Soc.*, **94**, 4329–4334, (2011).
- Wang, S.F., Zhang, J., Luo, D.W., Gu, F., Tang, D.Y., Dong, Z.L., Kong, L.B.: Transparent ceramics: processing, materials and applications, *Prog. Solid State Chem.*, **41**, 20–54, (2013).
- Hmood, F.J., Oelgardt, C., Görke, R., Heinrich, J.G.: Preparation of transparent microspheres in the system K_{0.5}Na_{0.5}NbO₃ by laser fusing, *J. Ceram. Sci. Tech.*, **04**, 41–48, (2013).
- Hmood, F.J., Guenster, J., Heinrich, J.G.: Sintering and piezoelectric properties of K_{0.5}Na_{0.5}NbO₃ glass microspheres, *J. Eur. Ceram. Soc.*, **35**, 4143–4151, (2015).
- Wang, X.B., Shen, Z.X., Hu, Z.P., Qin, L., Tang, S.H., Kuok M.H.: High temperature raman study of phase transitions in antiferroelectric NaNbO₃, *J. Mol. Struct.*, **385**, 1–6, (1996).
- Shanker, V., Samal, S.L., Pradhan, G.K., Narayana, C., Ganguli, A.K.: Nanocrystalline NaNbO₃, and NaTaO₃: Rietveld studies, Raman spectroscopy and dielectric properties, *Solid State Sci.*, **11**, 562–569, (2009).
- Rojac, T., Kosec, M., Malič, B., Holc, J.: Mechanochemical synthesis of NaNbO₃, *Mater. Res. Bull.*, **40**, 341–345, (2005).
- Mishra, S.K., Choudhury, N., Chaplot, S.L., Krishna, P.S.R., Mittal, R.: Competing antiferroelectric and ferroelectric interactions in NaNbO₃. Neutron diffraction and theoretical studies, *Phys. Rev. B.*, **76**, 024110, (2007).
- Dungan, R.H., Golding, R.D.: Metastable ferroelectric sodium niobate, *J. Am. Ceram. Soc.*, **47**, 73–76, (1964).
- Reznichenko, L.A., Turik, A.V., Kuznetsova, E.M., Sakhnenko, V.P.: Piezoelectricity in NaNbO₃ ceramics, *J. Phys.: – Condens. Mat.*, **13**, 3875, (2001).
- Carlsson, J.M., Hellsing, B., Domingos, H.S., Bristowe, P.D.: Theoretical investigation of the pure and Zn-doped α and δ phases of Bi₂O₃, *Phys. Rev. B.*, **65**, 205122, (2002).